

Solidification Crack Susceptibility of Aluminum Alloy Weld Metals (Report II)[†]

—Effect of Straining Rate on Cracking Threshold in Weld Metal during Solidification—

Yoshiaki ARATA*, Fukuhisa MATSUDA*, Kazuhiro NAKATA** and Kenzi SHINOZAKI

Abstract

The new Trans-Varestraint cracking test of Slow-Bending type has been developed in this study. The augmented-strain can be applied on the weld metal during welding with various straining rates in this cracking test.

The effect of the straining rate on the cracking threshold of the minimum augmented-strain required to cause cracking in the brittleness temperature range, BTR, during welding was investigated for Al-Mg and Al-Cu binary alloys and various commercially used aluminum alloys by means of Slow-Bending type Trans-Varestraint test (The SB Trans-Varestraint test).

Moreover, some metallurgical characteristics of weld metal, that is, the amount of eutectic products, the dihedral angle of eutectic products in grain boundaries and the grain size, were investigated.

Then, the effect of these metallurgical characteristics on the ductility in the weld metal in the BTR was discussed.

The main conclusions obtained are as follows:

- 1. The minimum augmented-strain required to cause cracking was raised at the lower temperature zone in the BTR as a decrease of straining rate. This phenomenon was observed in the weld metals of the alloys, the Mg content of which was more than about 3 wt% for Al-Mg alloys and the Cu content of which was more than about 5 wt% for Al-Cu alloys.*
- 2. The larger the dihedral angle of eutectic products on the grain boundary, the more the amount of eutectic products of weld metal and/or the smaller the grain size of weld metal, the larger the minimum augmented-strain required to cause cracking at the lower temperature zone in the BTR was.*

1. Introduction

In the previous report¹⁾, the effects of the kind and the amount of alloying element on the brittleness temperature range (BTR) and the ductilities of the weld metals in the BTR were investigated by Trans-Varestraint test for various aluminum alloys. As a result, it was made clear that the cracking threshold, that is, the minimum augmented-strain required to cause cracking (E_{min}) in the BTR was too low to be obtained by Trans-Varestraint test for each alloy except commercially pure aluminum.

However, the E_{min} of the weld metal in the BTR is very important factor for an index to decide the solidification crack susceptibility of aluminum alloys as well as the extent of the BTR.

Moreover, for the alloys, the BTR of which is so wide as aluminum alloys in the previous report¹⁾, it is considered that the value of E_{min} is affected a little by the straining rate during solidification due to extinguishment of the preceding augmented-strain. This will be obvious in slower straining rate. Therefore, E_{min} will be raised with a decrease of straining rate.

Consequently, in order to distinguish the E_{min} of

the weld metals in the BTR, The new type cracking test, which is named the Slow-Bending type Trans-Varestraint test (the SB Trans-Varestraint test), has been developed in this report. In this cracking test, the strain can be applied on the weld metal during welding with various straining rates. By using this cracking test, the effect of the straining rate on the E_{min} of the weld metal in the BTR for various aluminum alloys has been investigated and then the curves for the cracking threshold are determined.

Then the effects of the kind and the amount of the alloying elements and the additional refining elements on the E_{min} are also investigated.

On the basis of the curve for cracking threshold, the solidification crack susceptibility is decided for various aluminum alloys as an index of the CST²⁾.

On the other hand, it is considered that the eutectic products with lower melting temperature largely affect the solidification crack susceptibility. Therefore, the properties of the eutectic products, that is, the dihedral angle and the amount of eutectic products, are investigated to be related to the ductility of the weld metal in the BTR.

[†] Received on April 5, 1977

* Professor

** Graduate student

2. Materials Used and Experimental Procedures

2.1 Materials used

The materials used are 6 mm in thickness of commercially used aluminum alloys and Aluminum-Magnesium (Al-Mg) and Aluminum-Copper (Al-Cu) binary alloys. Chemical compositions of materials used are shown in Tables 1 and 2. Among of commercially used aluminum alloys, 1070 is commercially pure alloy, 5052, 5154 and 5083 are Al-Mg alloys, 2017 and 2219 are Al-Cu alloys and 7N01 is Aluminum-Zinc-Magnesium (Al-Zn-Mg) system alloy. Next, the Al-Mg and Al-Cu binary alloys, Mg or Cu content of which was varied from about 0.5 to 5 wt%, respectively,

were experimentally melted. The process of the production is the same as the previous report¹⁾.

Moreover, for the purpose of grain refinement of weld metal, zirconium (Zr), titanium (Ti) and boron (B) were added slightly on the base alloys. In the case of 5083, one was added with Zr about 0.17 wt% and the other was added with Ti and B about 0.01 to 0.02 wt% and 0.002 to 0.003 wt%, respectively. Among of Al-Mg binary alloys, that is, alloy (3) and (5), Ti and B were added about 0.01 and 0.002 wt%, respectively.

All of the materials were used under annealed condition.

Table 1 Chemical compositions of commercial aluminum alloys used.

Material	Chemical composition (wt%)									
	Cu	Si	Fe	Mn	Mg	Zn	Cr	Ti	Zr	B
1070-0	0.02	0.10	0.33	<0.01	<0.01	<0.01	<0.01	0.04	—	—
2017-0	3.80	0.47	0.43	0.47	0.44	0.11	0.03	0.02	—	—
2219-0	6.32	0.08	0.11	0.33	<0.01	0.04	<0.01	0.04	—	—
7N01-0	0.10	0.07	0.21	0.48	1.22	4.00	0.08	0.04	0.11	—
5052-0	0.04	0.09	0.19	0.01	2.50	0.01	0.15	<0.01	—	—
5154-0	0.02	0.11	0.25	0.06	3.50	<0.01	0.23	0.03	—	—
5083-0	0.03	0.10	0.18	0.79	4.44	0.02	0.10	0.02	<0.01	—
5083*-0	0.03	0.10	0.18	0.79	4.44	0.02	0.10	0.02	—	0.003
5083**-0	0.03	0.10	0.18	0.79	4.44	0.02	0.10	0.02	0.17	—

Table 2 Chemical compositions of aluminum binary alloys used.

Material	Designation	Chemical composition (wt%)								
		Cu	Si	Fe	Mn	Mg	Zn	Cr	Ti	B
Commercially Pure Al	1	<0.01	0.06	0.15	<0.01	<0.01	0.01	<0.01	<0.01	—
Al-Mg binary alloys	2	<0.01	0.06	0.15	<0.01	0.51	0.01	<0.01	<0.01	—
	3	<0.01	0.06	0.15	<0.01	0.99	0.01	<0.01	<0.01	—
	3*	<0.01	0.06	0.14	<0.01	1.02	0.01	<0.01	0.013	0.0021
	4	<0.01	0.06	0.15	0.01	1.72	0.01	<0.01	<0.01	—
	5	<0.01	0.06	0.15	0.02	3.03	0.01	<0.01	<0.01	—
	5*	<0.01	0.06	0.14	0.01	3.02	0.01	<0.01	0.011	0.0019
Al-Cu binary alloys	6	<0.01	0.06	0.14	0.01	4.88	<0.01	<0.01	<0.01	—
	A	0.45	0.06	0.13	<0.01	0.01	0.01	<0.01	<0.01	—
	B	0.84	0.06	0.15	<0.01	0.01	0.01	<0.01	<0.01	—
	C	2.05	0.06	0.18	0.01	0.02	0.01	<0.01	<0.01	—
	D	3.00	0.07	0.19	0.01	0.02	0.01	<0.01	<0.01	—
	E	4.96	0.07	0.22	0.01	0.04	0.03	<0.01	<0.01	—

2.2 Method for macroscopic and microscopic investigations of characteristics of weld metal structure

2.2.1 Measurement of grain size in weld metal

The specimen was mechanically polished and then electrolytically etched in Barker's reagent using a pure aluminum plate for cathode.

Then the grain size in weld metal was measured with the line-intercept method³⁾ which was performed by using an optical microscope with crossed polarizer with an eyepiece with 400 points of intersection meth. The magnification for the observation was $\times 100$ and $\times 400$ and the position of measurement was from 50 to 100% in Y(%) which is the parameter indicating the position in weld bead and 0 and 100% show the fusion boundary and the center of weld bead, respectively.

2.2.2 Measurement of dihedral angle of eutectic products at grain boundary in weld metal

The dihedral angle of eutectic products at the grain boundary in weld metal was measured as the angle, θ , between two tangent lines which were drawn at the tip of arbitrary eutectic products on the photomicrograph of magnification $\times 1500$ as shown in Fig. 1.

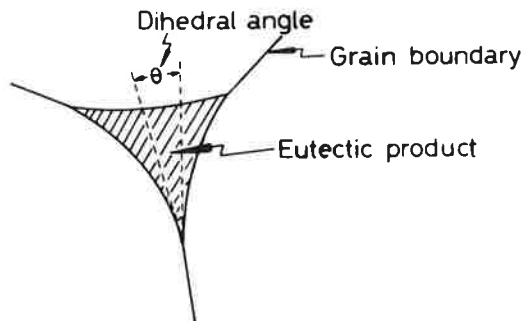


Fig. 1 Method for measurement of the dihedral angle of eutectic products in the weld metal.

The number of samples is about 100. Then the angle measured was arranged in the cumulative curve and angle where the frequency was 50% was adopted as the dihedral angle⁴⁾. This dihedral angle seems to correspond to that of remaining liquid in the last stage of solidification, that is, near the lowest temperature of the BTR.

2.2.3 Measurement of amount of eutectic products in weld metal

The measurement of the amount of eutectic products in the weld metal was performed with point-counting method⁵⁾ as the same manner described in the previous report¹⁾.

3. Principle of the Slow-Bending Type Trans-Varestraint Cracking Test Method (The SB Trans-Varestraint Test) and Its Use for Evaluation of Solidification Crack Susceptibility

3.1 The SB Trans-Varestraint test

The general appearance of the SB Trans-Varestraint apparatus is shown in Photo. 1 and the simplified sketch of the operation of it is shown in Fig. 2. This

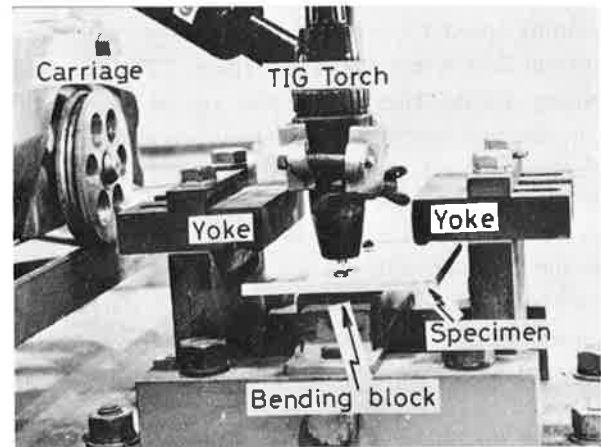


Photo. 1 Close-up view of the Slow-Bending type Trans-Varestraint apparatus

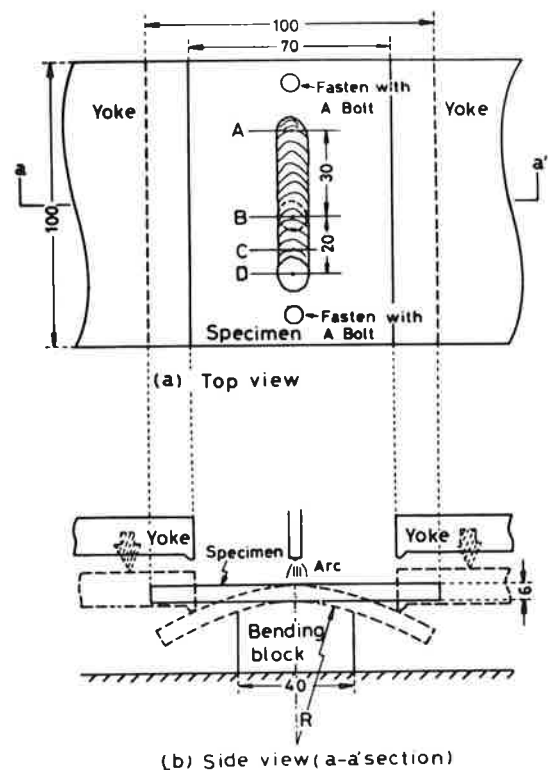


Fig. 2 Simplified sketch of operation of the Slow-Bending type Trans-Varestraint cracking tester.

cracking test apparatus is almost the same as the Trans-Varestraint testing apparatus used in previous report¹⁾. It is, however, different in the point where the bending speed applied on the specimen is widely variable by an use of a variable speed electric motor. In Fig. 2, using a test specimen of 100 mm long by 100 mm wide with thickness of 6 mm, which is fixed on the bending brock by two bolts in distance of 80 mm, a conventional TIG arc melt-run weld (AC) is done from points (A) to (D) with the welding condition of welding speed 100 mm/min, arc voltage 18 V and arc current 230 A but 240A for 7N01, 220A for Al-Mg binary alloys. Then, when the arc passes the point (B), the two loading yokes which are attached to the electric motor begin to bend the specimen downward by descending with the constant speed. The bending process continues as long as the applied strain reaches to the ultimate value previously decided and then stops with cutting off the electric circuit of electric motor automatically. Meanwhile, the arc travels steadily onward and is subsequently interrupted at the point (D).

After the cracking test, the surface of the SB Trans-Varestraint tested specimen is examined at $\times 6$ to $\times 70$ magnification for evidence of solidification crack in weld metal around the point (B) where bending was began to start.

The straining rate and the augmented-strain applying on the specimen surface were measured by each base metal without welding operation with a strain gage stucked on specimen surface and a dynamic strain meter. Figure 3 shows an example for the variation of augmented-strain against time after the start of bending the specimen from the horizontal state. In

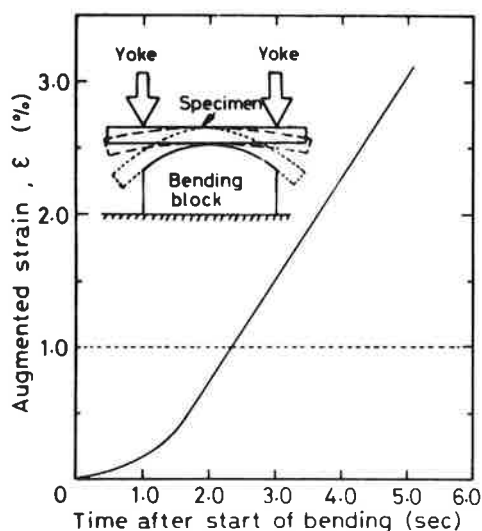


Fig. 3 An example of dynamic variation of strain applied on specimen surface.

Fig. 3, it is cleared that straining rate is almost constant as the augmented-strain is more than about 1%. Therefore, in order to apply the strain on the specimen surface with constant straining rate during cracking test, the prestrain of 1% was applied on the specimen before cracking test.

The augmented-strain can be varied to any desired value by adequately selecting the distance of descent of the bending yokes.

3.2 Dynamic straining rate applied on specimen surface during the SB Trans-Varestraint test

The straining rate measured by a strain gage described in 3.1 is the value on the specimen surface without welding. Therefore, it may be different for the one applied on the surface of weld metal during actual cracking test. So, comparing the both values in the above mentioned, the straining rate applied on the weld metal surface during cracking test was measured by means of camera method^{6),7)}.

In advance of welding, two micro vickers' marks (load 50 Kg) indented on the either side of weld bead which will pass there with a distance of about 12 mm were continuously taken photographs by the camera with the speed of 5 frame/sec and with about $\times 1.1$ magnification during cracking test. Then, the variation of the distance of the two marks against time was measured to 1/100 mm on the film using film projector of $\times 20$ magnification. The typical examples of instantaneous strains during cracking test are shown in round and triangle marks in Fig. 4. The straining rate measured by the strain gage are also shown as solid lines. The both results have comparatively good correlations. Consequently, in this study, the straining rate and augmented-strain measured by strain gage without welding have been adopted.

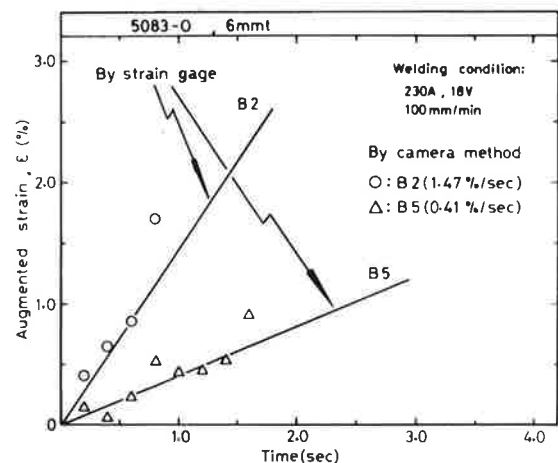


Fig. 4 An example of measurement results for straining rate by "camera method".

3.3 Measurement of minimum augmented-strain required to cause cracking (E_{min})

In the SB Trans-Varestraint test, the cracking threshold curve for the E_{min} in the weld metal can be obtained as the following manner. For example, in the case of alloy 2017, as shown in Fig. 5, each

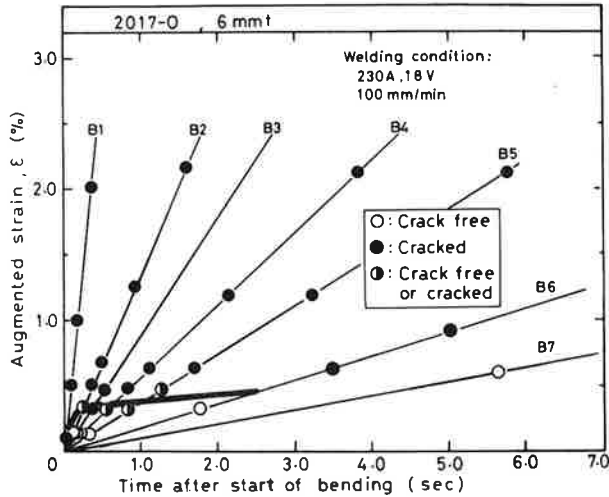


Fig. 5 Effect of the straining rate on the minimum augmented-strain required to cause cracking in the weld metal of 2017.

minimum augmented-strain required to cause cracking (E_{min}) are determined on various straining rates as shown by the lines B1 to B7 which is no longer cracking and then the cracking threshold line is drawn by a bold line. It is, however, necessary for discussion on the ductility of the weld metal in the BTR to relate the both indices, E_{min} and critical strain rate required to cause cracking \dot{E}_c against temperature.

So, the temperature distribution along the center line of weld bead was also measured with a 0.5 mm dia. W+5% Re/W+26%Re termocouples.

An example of the cooling curve for 2017 weld metal is shown in Fig. 6.

From the combination of Fig. 5 with Fig. 6, the curve for cracking threshold is obtained against temperature in weld metal as shown in Fig. 7 schematically. Figure 7(a) shows the straining rate which indicates the variation of augmented-strain against time, Fig. 7(b) shows the cooling curve in the center of weld bead and Fig. 7(c) shows the straining rate against temperature. For example, in Fig. 8, the curves shown as B1 to B7 correspond to the straining rate against time, B1 to B7, in Fig. 6. Moreover, the curve drawn by a bold line in Fig. 8 shows the variation of E_{min} against temperature, that is, the curve of cracking threshold in the weld metal against temperature. The characteristic of this cracking threshold curve is discussed in 4.2.

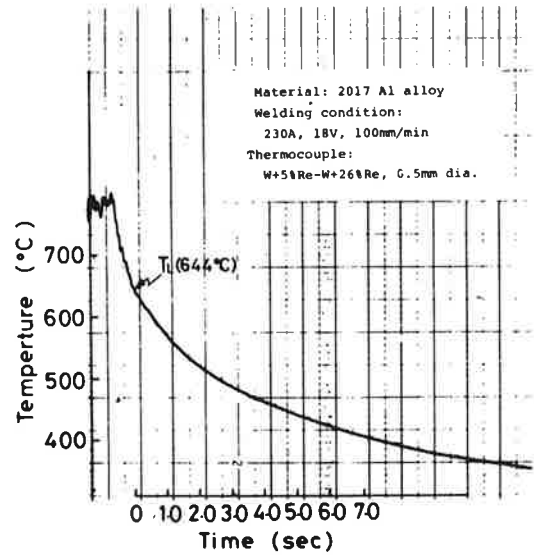


Fig. 6 An example for cooling curve along weld center during the cracking testing.

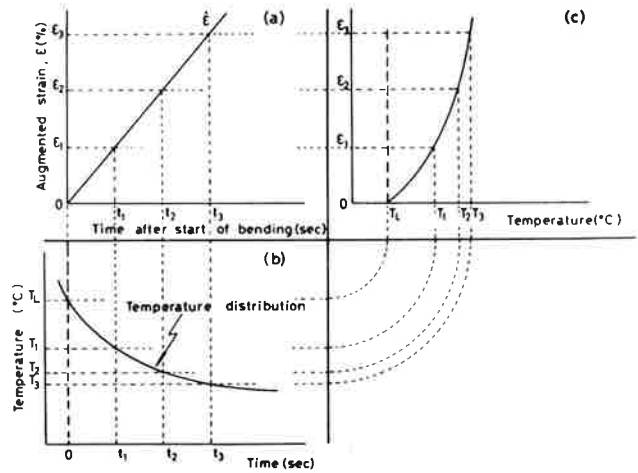


Fig. 7 Illustration of procedure for decision of cracking threshold curve in the weld metal using dynamic straining rate and temperature distribution.

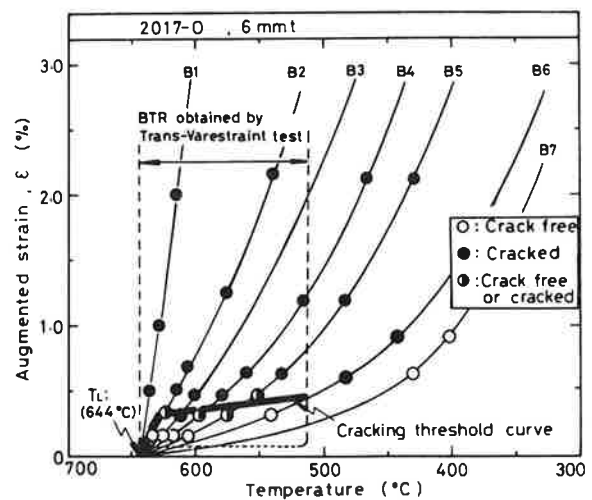


Fig. 8 Cracking threshold curve in the weld metal of 2017.

4. Result and Discussion for Cracking Threshold Curve (E_{min} Curve) of Various Aluminum Alloy Weld Metals

4.1 Effect of straining rate on E_{min} in weld metal

The relations between straining rate and E_{min} are shown in Fig. 9 through Fig. 13. The curves drawn as the bold lines indicate the cracking threshold, the lower zones of which are crack free respectively.

The arrows at each end of the bold lines indicate the critical straining rate required to cause cracking ($\dot{\epsilon}_c$). Figure 9 shows for various commercially used

aluminum alloys. In Fig. 9, in the case of 1070, the E_{min} shows a constant value of about 0.15%, although the straining rate is not so widely changeable due to its high $\dot{\epsilon}_c$ comparing with the other alloys. On the contrary, for the other alloys, the values of E_{min} are affected with a decrease of straining rate from the highest rate of usual Trans-Varestraint test. As the straining rate decreases, the E_{min} is strongly increased for 5xxx system of Al-Mg alloys. Especially for 5083, the rate of increase of the E_{min} for the decrease of straining rate is very large. On the other hand, for 2017 of Al-Cu system alloy and 7N01 of Al-Zn-Mg

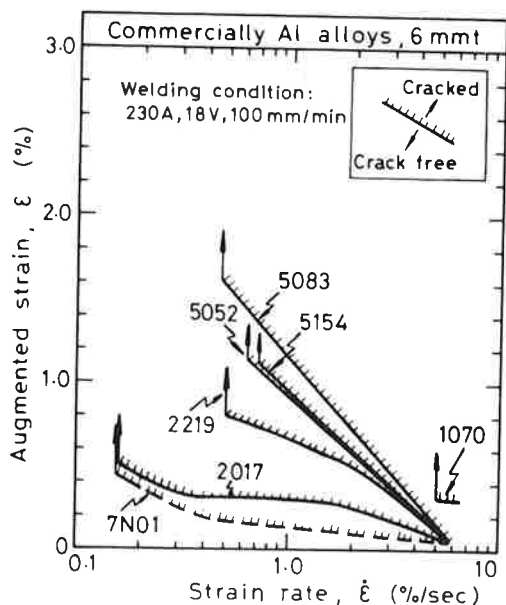


Fig. 9 Effects on straining rate on cracking threshold in the weld metals for commercially used aluminum alloys.

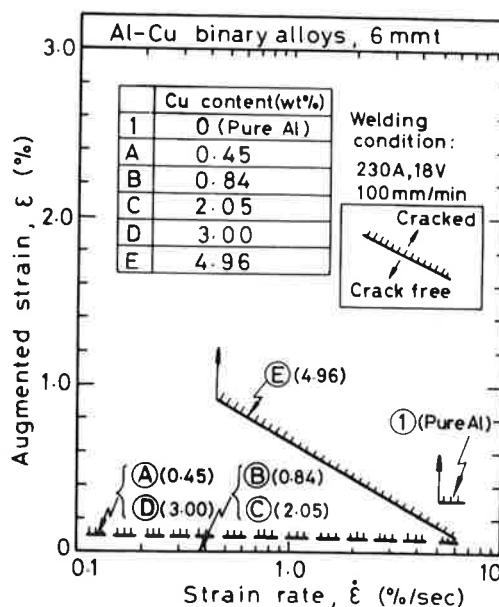


Fig. 11 Effects of straining rate on cracking threshold in the weld metals for Al-Cu binary alloys.

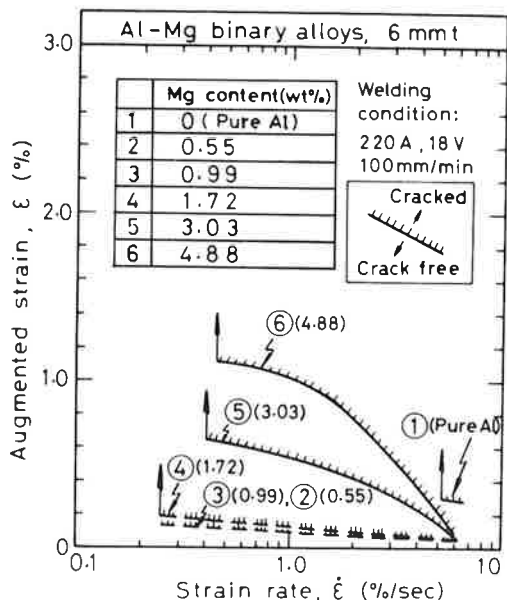


Fig. 10 Effects of straining rate on cracking threshold in the weld metals for Al-Mg binary alloys.

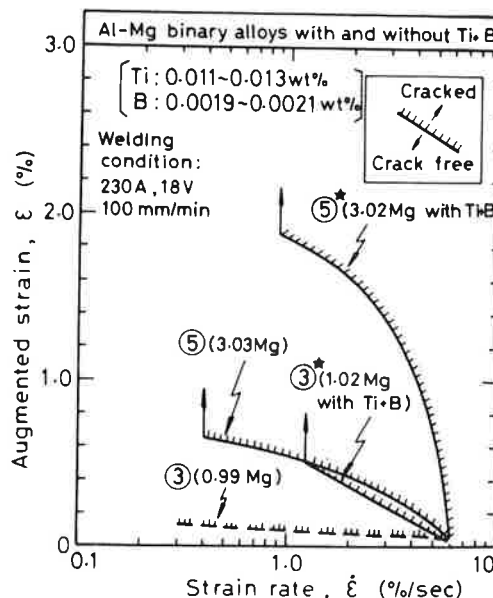


Fig. 12 Effects of additional refining element on cracking threshold in the weld metal for Al-Mg binary alloys.

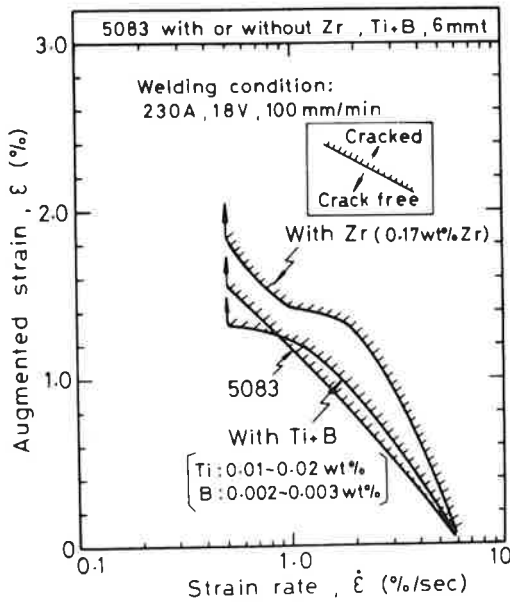


Fig. 13 Effect of additional refining elements on the cracking threshold in the weld metal for 5083.

system alloy, the E_{min} does not increase so much as for Al-Mg system alloys, though the E_{min} of 2219 is comparatively raised.

Next, Fig. 10 and 11 show the results for Al-Mg and Al-Cu binary alloys, respectively. As the alloy (1) corresponds to commercially pure aluminum, the E_{min} and \dot{E}_c are almost equal to those of 1070. For Al-Mg binary alloys as shown in Fig. 10, in the case of alloys, Mg content of which is less than about 1.7 wt%, the E_{min} does not increase even in the very slow straining rate, so that, especially for the alloys, Mg content of which is less than about 1.0 wt%, the \dot{E}_c are too small to be determined in this investigation.

However, as the Mg content of alloy is increased more than about 3 wt%, the E_{min} is increased with a decrease of straining rate and the more the Mg content is, the more remarkable these tendencies become.

On the other hand, as shown in Fig. 11 for Al-Cu binary alloys, only for alloy (E) of about 5 wt% Cu, the E_{min} is increased with a decrease of straining rate. On the contrary, the E_{min} for the alloys, Cu content of which is less than about 3 wt%, is very low values independently to the straining rate, so that the \dot{E}_c can not be determined in this investigation.

Furthermore, Fig. 12 and 13 show the additional refining elements as Ti, B and Zr on the E_{min} . In Fig. 12, for the Al-Mg binary alloys, the E_{min} of the alloys added Ti together with B, that is, Ti+B, is increased more than those of the alloys without addition. Especially for Al-3 wt% Mg alloy, this tendency becomes remarkable. Moreover, the \dot{E}_c is also increased with addition of Ti+B.

In the case of 5083 as shown in Fig. 13, it seems that the addition of Zr (about 0.17wt%) increases the E_{min} more than that of usual 5083 but the effect of the addition of Ti+B on the E_{min} is not so obvious.

As a result, it has been clear that the E_{min} of aluminum alloys is depended on the straining rate and the degree of its dependency of the E_{min} against the straining rate is largely varied with the kind and the amount of alloying element as the \dot{E}_c does.

4.2 Cracking threshold curve in the BTR

The temperature variation during applying the strain in cracking test is not taken into consideration in the data shown in Fig. 9 through Fig. 13. Consequently, the relation between the E_{min} or the \dot{E}_c and temperature was discussed here.

4.2.1 Commercially used aluminum alloys

The cracking threshold curves are shown in Fig. 14 through Fig. 17. In these figures, the curves drawn

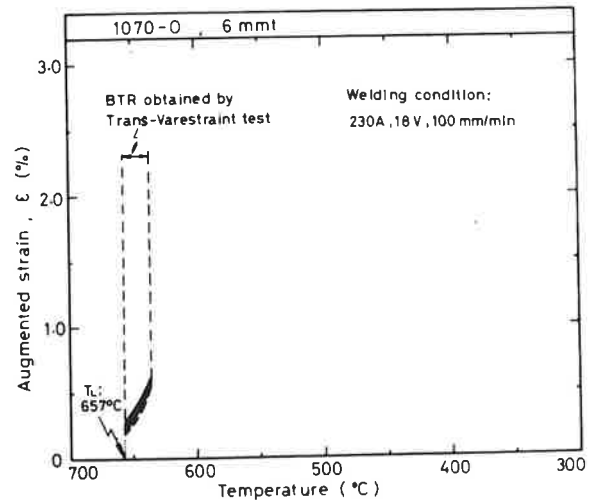


Fig. 14 The cracking threshold curve in the weld metal of commercially pure aluminum alloy.

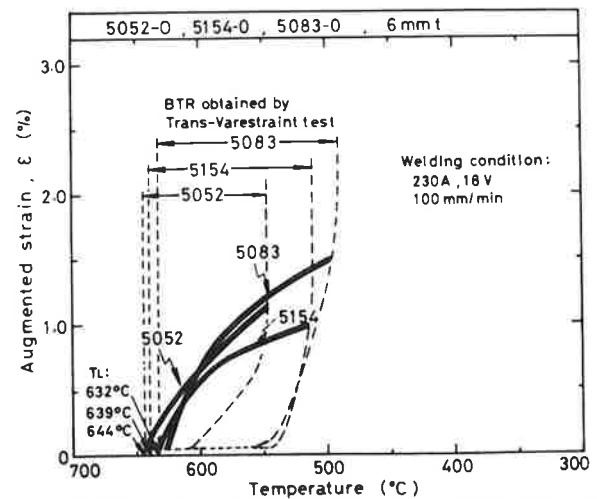


Fig. 15 The cracking threshold curves in the weld metals of 5052, 5154 and 5083 commercially used Al-Mg system alloys.

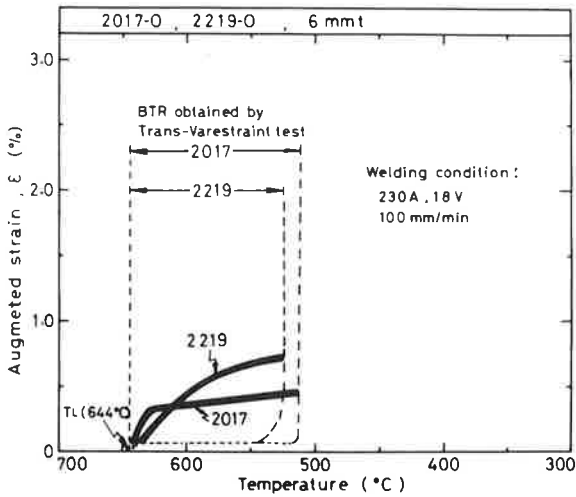


Fig. 16 The cracking threshold curves in the weld metals of 2017 and 2219 commercially used Al-Cu system alloys.

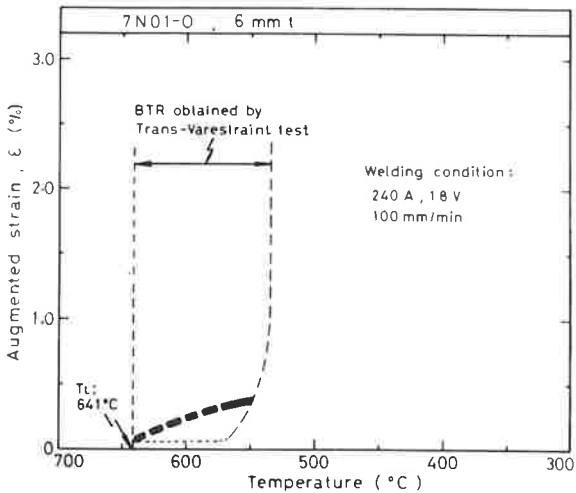


Fig. 17 The cracking threshold curve in the weld metal of 7N01 commercially used Al-Zn-Mg system alloy.

the SB Trans-Varestraint test are different from the cracking curves by Trans-Varestraint test.

As shown in Fig. 15, for 5052, 5154 and 5083 of Al-Mg system alloys, the cracking threshold is largely increased in the lower temperature zone as the decrease of straining rate, especially in 5083, Mg content of which is the highest in the above alloys.

On the other hand, from Fig. 16 and Fig. 17 for 2017 and 2219 of Al-Cu system alloys and 7N01 of Al-Zn-Mg system alloy, the cracking threshold is less increased than that of Al-Mg system alloys in the lower temperature zone as the decrease of straining rate. Especially for 7N01, the cracking threshold is only increased a little near the lowest temperature zone in the BTR. Moreover, comparing the cracking threshold curve of 2219 for that of 2017, the E_{min} in the lowest temperature zone in the BTR for 2219, Cu content of which is more than that of 2017, is larger than that of 2017.

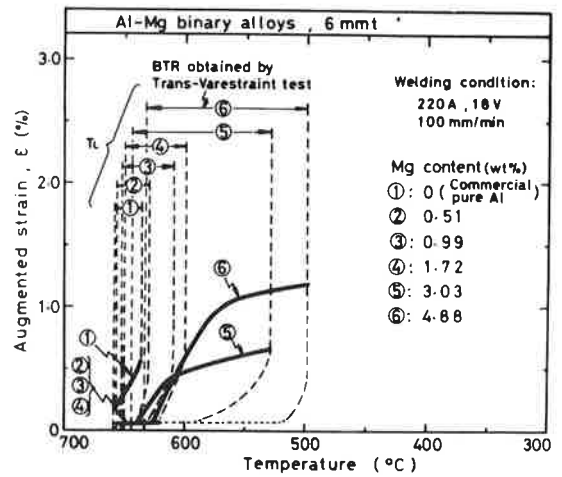


Fig. 18 The cracking threshold curves in the weld metals of Al-Mg binary alloys.

by the broken lines show the cracking curves in the weld metal obtained by the Trans-Varestraint test in the previous report¹⁾.

The curves of 1070 are shown in Fig. 14. In case of 1070, it is obvious that the BTR is very narrow and the ductility is high.

Moreover, the cracking threshold curve (drawn by bold line) obtained by the SB Trans-Varestraint test is almost equal to it obtained by Trans-Varestraint test (drawn by broken line).

On the contrary, in case of the other alloys in Fig. 15 through Fig. 17, the BTRs of which are wider than that of 1070, the cracking threshold curves show very small value less than 0.1% in the higher temperature zone of the BTR but tend to be increased in the lower temperature zone as the decrease of straining rate. Consequently, the cracking threshold curves by

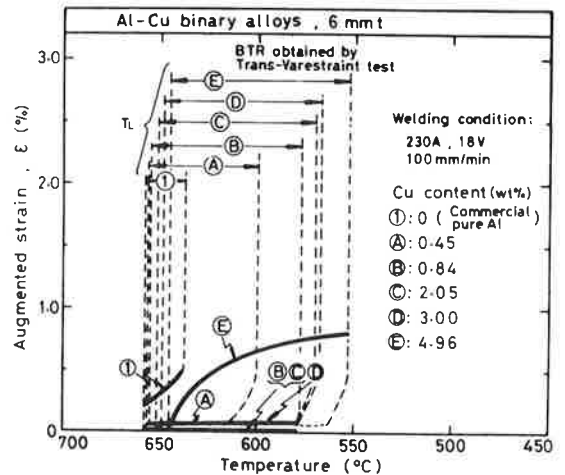


Fig. 19 The cracking threshold curves in the weld metals of Al-Cu binary alloys.

4.2.2 Al-Mg and Al-Cu binary alloys

Figures 18 and 19 show the cracking threshold curves as the bold lines for Al-Mg and Al-Cu binary alloys, respectively. In Fig. 19 as regards to alloy (B) and (C), Cu contents of which are about 0.8 and 2 wt%, respectively, the cracking occurred only with bead-on-plate welding. So that, the ductility of these alloys, which are below zero, are shown as zero in Fig. 19 for convenience. From Fig. 18 and Fig. 19, it is made clear that the E_{min} in the higher temperature zone in the BTR is very low value for binary alloys except alloy (I) which is almost equal to 1070.

Moreover, it is observed that the cracking threshold is inclined to increase in the lower temperature zone in the alloys, the alloying content of which is more than 3 wt% Mg for Al-Mg and 5 wt% Cu for Al-Cu binary alloys. Especially in Al-Mg binary alloys, the cracking threshold become larger as an increase of Mg content.

On the contrary, in case of Al-Cu alloys less than 3 wt% Cu, the cracking threshold shows a low value still in the lower temperature zone of the BTR and then almost equal to the value of the E_{min} obtained by the Trans-Varestraint test drawn by the broken line. Comparing the cracking threshold of these two binary alloys in the same alloying content, that of the Al-Mg binary alloy is higher than that of Al-Cu binary alloys in lower temperature zone in the BTR. This tendency is also observed in the case of the commercially used aluminum alloys.

4.2.3 Alloy with additional refining element

The cracking threshold curves of the alloys with and without additional refining elements are shown in Fig. 20 and 21, respectively.

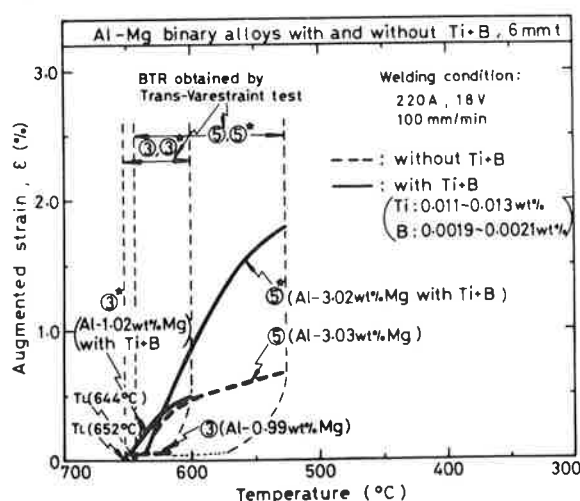


Fig. 20 The effects of the additional refining elements, titanium and boron on the cracking threshold curves in the weld metals of Al-1 and -3 wt% Mg binary alloys.

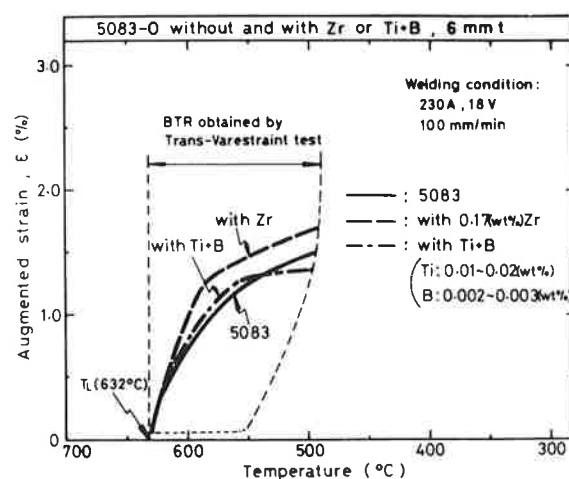


Fig. 21 The effects of the additional refining elements, zirconium, titanium and boron on the cracking threshold curve in the weld metals of 5083 commercially used Al-Mg system alloy.

Figure 20 shows the cracking threshold curves of alloys (3) (1 wt% Mg) and (5) (3 wt% Mg) with and without Ti+B. As shown in Fig. 20, though the E_{min} is very low in the higher temperature zone in the BTR for each alloy, those of the alloys with Ti+B are increased to higher values than those without Ti+B in the lower temperature zone in the BTR. Especially for alloy (5), the effect of addition of Ti+B on an increase of the curve is remarkable.

As the same manner, for the alloy 5083 as shown in Fig. 21, addition of 0.17 wt% Zr increases the E_{min} in the lower temperature zone of the BTR more than that of 5083 without Zr but not so remarkable in the case of addition of Ti+B.

4.3 Evaluation of solidification crack susceptibility of aluminum alloy weld metals

By one of the authors, the critical strain rate for temperature drop (CST)²⁾, which is defined as the inclination of tangential line to the ductility curve from the highest boundary temperature of the BTR, that is, the effective liquidus temperature, was proposed as the index for evaluation of solidification crack susceptibility. However, as described in this report of aluminum alloys, the BTR of which is relatively wider as compared with commercial steels, the ductility curve is partly affected by the straining rate, especially in low straining rate, due to recovery of the preceding strain. Therefore, in case of this, the ductility curve should be substituted to the cracking threshold curve in this report. Accordingly the value of the CST in alloy should be also determined using the cracking threshold curve and \dot{E}_c value.

The CST for commercially used aluminum alloys

in this investigation are shown in **Table 3**. In general, the larger the CST, the better the solidification crack susceptibility of the weld metals. So that, an order of solidification crack susceptibility is arranged as the inverse order of CST value, as follows.

Table 3 CST values obtained from the cracking threshold curves in the weld metals for commercially used aluminum alloys

Commercially Al alloys	CST ($\times 10^{-4}/^{\circ}\text{C}$)
1 0 7 0	3.50
5 0 5 2	1.17
5 0 8 3	1.13
5 1 5 4	0.81
2 2 1 9	0.70
7 N 0 1	0.42
2 0 1 7	0.37

1070 < (5052, 5083) < 5154 < 2219 < (7N01, 2017)

Meanwhile, the result of measurement of the CST for binary alloys is shown in **Table 4**. Also, the **Fig. 22** shows the relation between the CST in Table 4 and the amounts of alloying elements.

Table 4 CST values obtained from the cracking threshold curves in the weld metals for Al-Mg and Al-Cu binary alloys

Designation	CST ($\times 10^{-4}/^{\circ}\text{C}$)	
Pure Al	1	3.50
Al-Mg binary alloys	2 (0.51wt% Mg)	0 to 0.63
	3 (0.99 ")	0 to 0.45
	4 (1.72 ")	0 to 0.33
	5 (3.03 ")	0.50
	6 (4.88 ")	0.83
Al-Cu binary alloys	A (0.45wt% Cu)	0 to 0.13
	B (0.84 ")	0
	C (2.05 ")	0
	D (3.00 ")	0 to 0.10
	E (4.96 ")	0.86

From **Fig. 22**, the values of the CST are very small as the Mg content is less than about 2 wt% for Al-Mg binary alloys and Cu content is less than about 3 wt% for Al-Cu binary alloys, but for the former they gradually increase as the Mg content increases more than 3 wt% and for the latter they abruptly increase as the Cu content increases to about 5 wt%.

These results show that the solidification crack susceptibility in the weld metal of Al-Mg and Al-Cu

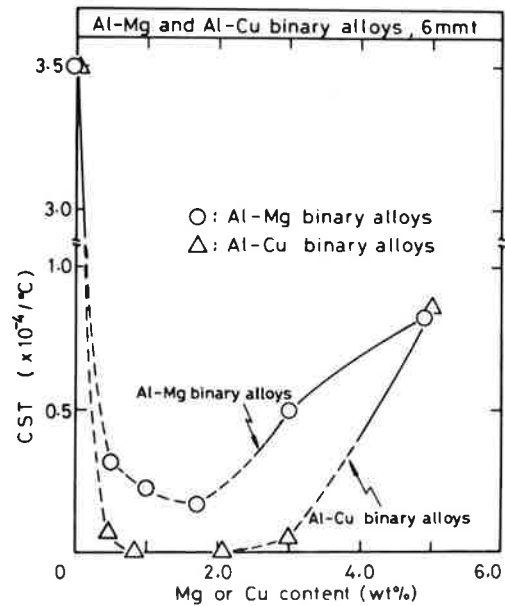


Fig. 22 The effects of the alloying content on the critical strain rate for temperature drop (CST) for the weld metals of Al-Mg and Al-Cu binary alloys.

binary alloys become better as the increase of the alloying contents which are more than about 3 wt% Mg and 5 wt% Cu for Al-Mg and Al-Cu binary alloys, respectively.

Moreover, it seems that these tendencies are almost equal to the qualitative tendencies for crack susceptibility in the weld metal as well known^{(8), (9)}.

Table 5 shows the CST values of the alloys with and without additional refining element for comparison. In addition of Ti+B, the CST value increases about two times as large as usual Al-1.0 wt% Mg alloy and about three times as large as usual Al-3.0 wt% Mg alloy.

Meanwhile, for 5083, there is no remarkable effect of the addition of Zr or Ti+B on the CST, though it increases a little with the addition of Zr. The reason in the above seems that the CST values of 5083 is very

Table 5 CST values obtained from the cracking threshold curves in the weld metals with or without additional refining elements for 5083 and Al-Mg binary alloys

Material	CST ($\times 10^{-4}/^{\circ}\text{C}$)	
5 0 8 3	Not added	1.13
	Zr added	1.28
	Ti+B added	1.00
Al-1.0(wt%)Mg	Not added	0 to 0.45
	Ti+B added	0.87
Al-3.0(wt%)Mg	Not added	0.50
	Ti+B added	1.45

large even in case of usual alloy. As a result, the solidification crack susceptibility evaluated by the CSTs obtained from the cracking threshold curves in this investigation, in general, seems to agree with it previously well known qualitatively for various aluminum alloys.

4.4 Effect of metallurgical factor on cracking threshold curve

The tendency of increase in the E_{min} in the lower temperature zone against slow straining rate is largely different from kind of alloy and amount of alloying element in alloy. It is well known that the dihedral angle and the amount of the eutectic products and the grain size of weld metal are main metallurgical factors which largely affect on the solidification crack susceptibility. Therefore, the effects of these metallurgical factors on the cracking threshold curves were investigated here.

Photo. 2 (a) and (b) show the microstructures ($\times 400$)

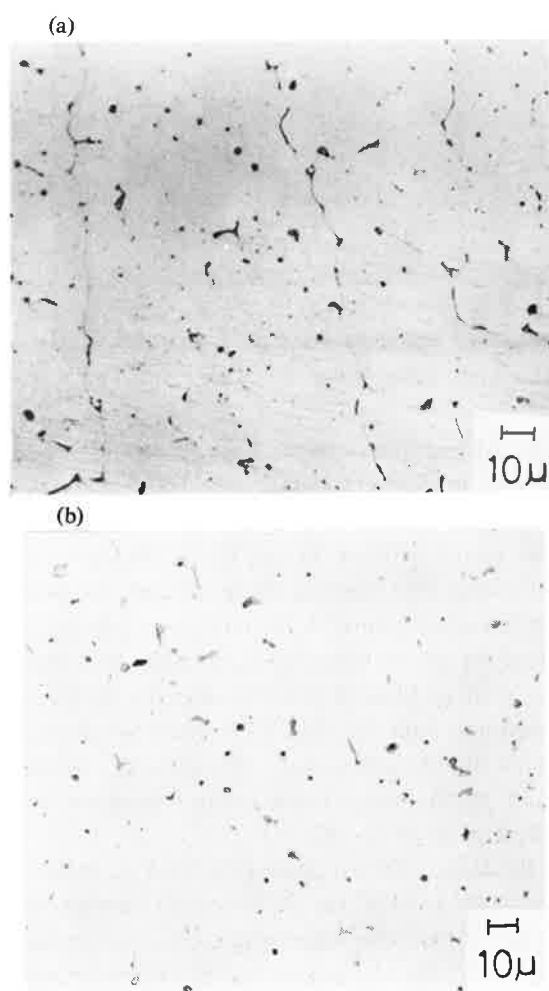


Photo. 2 Eutectic products in weld metal
(a) 7N01
(b) 5083

of the weld metals of commercially used aluminum alloys of 7N01 and 5083, respectively.

In Photo. 2(a) for 7N01, the film-like eutectic products are observed along the grain boundaries. On the contrary, for 5083 as shown in Photo. 2(b), the eutectic products, the shape of which are almost globular, are scattered in grain boundaries. The E_{min} of alloy 7N01 in the lower temperature zone with slow straining rate is very low but the E_{min} of alloy 5083 is much higher than the former.

Next, **Photo. 3** shows weld metals of Al-Mg binary alloys. Photo. 3 (a), (b) and (c) correspond to the alloy (3) (1 wt% Mg), alloy (5) (3 wt% Mg) and alloy (6) (5 wt% Mg), respectively. In Photo. 3 among of these alloys, the total amount of eutectic products are not largely different for each other. However, it is obvious that the shape of eutectic products at the grain boundary is varied from film-like to globular one as the increase of Mg content. The E_{min} in the lower temperature zone in the BTR is increased with an increase of Mg content as previously mentioned.

As a result, it seems that the shape of eutectic products largely affects on the E_{min} in the lower temperature zone in the BTR. So, in order to evaluate the shape of eutectic products, the dihedral angle of it in the grain boundary of weld metal, which is considered to indicate the value of it near the temperature of lower boundary of the BTR has been measured for each alloy, since the solidification cracking always occurs in the grain boundary in the weld metal.

Moreover, **Photo. 4** shows the typical examples of the weld metal of Al-Cu binary alloys. Photo. 4(a), (b) and (c) correspond to alloy (B) (0.8 wt% Cu), (D) (3 wt% Cu) and (E) (5 wt% Cu), respectively. From Photo. 4, the shapes of eutectic products are almost film-like for each alloy differing from the case of Al-Mg binary alloys. On the contrary, the amount of eutectic products increases with an increase of Cu content. As the E_{min} in lower temperature zone of the BTR is largely increased in the case of alloy (E), it seems that the amount of eutectic products also affect on the cracking threshold curve.

Figure 23 shows the relation between the dihedral angle and the amount of eutectic products measured in this investigation. The E_M in Fig. 23 indicates the maximum value of E_{min} in the cracking threshold curve. From Fig. 23, it is obvious that the E_M is mainly depended on the dihedral angle.

Next, **Photo. 5** shows the weld metal of alloy (5) (3 wt% Mg) with and without additional element of Ti+B. The grain sizes in the weld metal are remarkably refined to small size by the addition of Zr or Ti+B

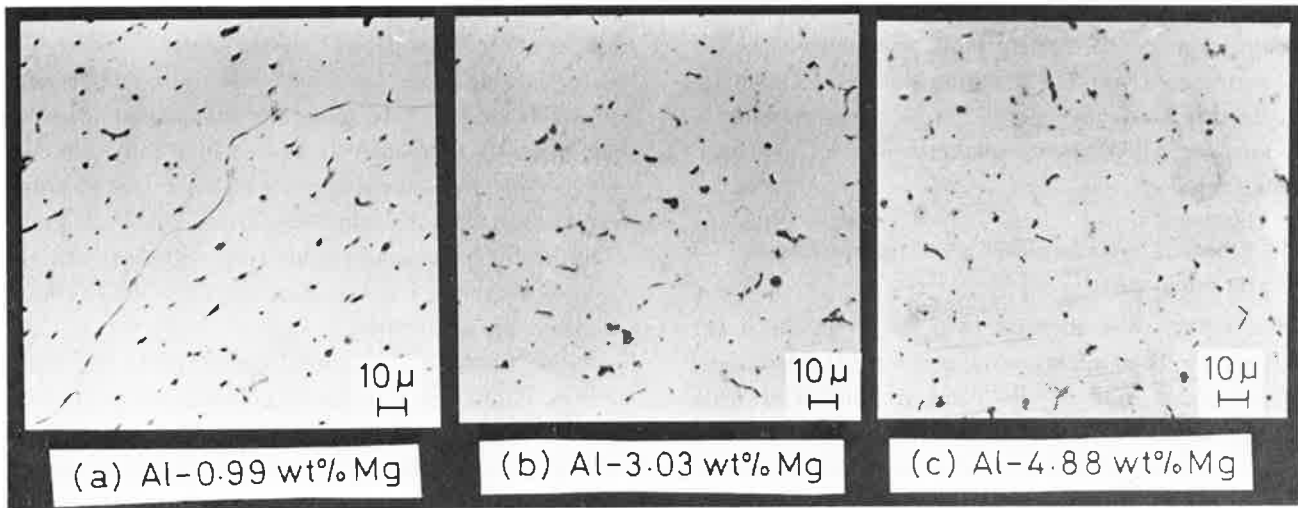


Photo. 3 Eutectic products in weld metal for Al-Mg binary alloys.

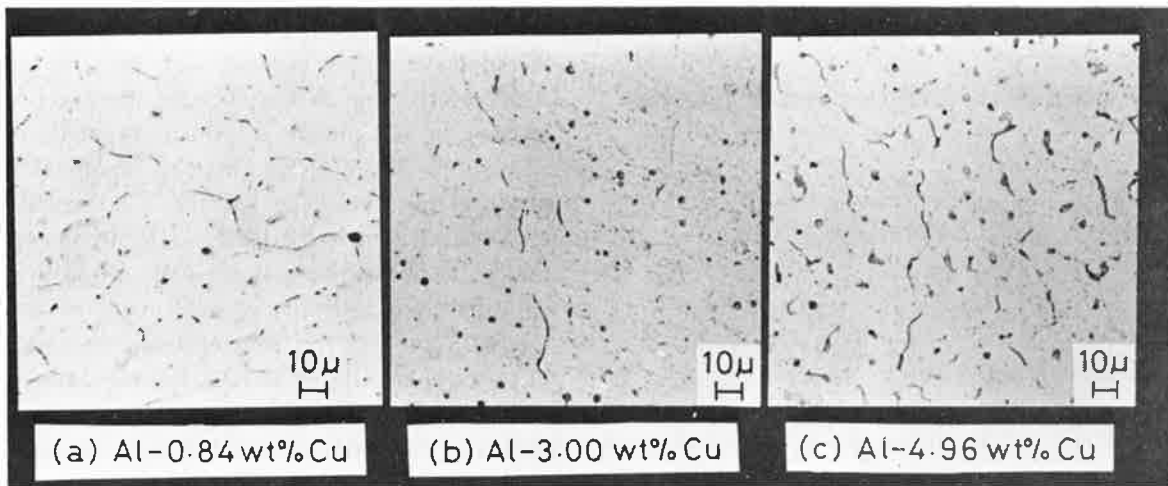


Photo. 4 Eutectic products in weld metal for Al-Cu binary alloys.

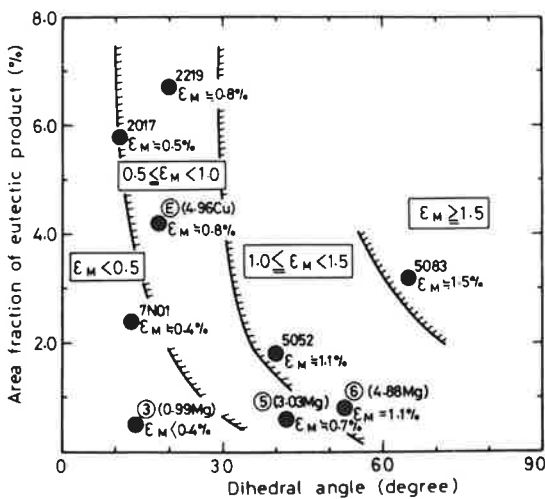


Fig. 23 The effects of the dihedral angle of eutectic products in the grain boundary and the amount of eutectic products indicated as the area fraction of them on the maximum value of the E_{min} in the cracking threshold curve.

for the Al-Mg binary alloys and 5083, and the mean grain sizes in the weld metals measured are about 40μ , that is, about a half or a quarter times as large as those of the alloys without Zr or Ti+B. Meanwhile, the amount and the dihedral angle of eutectic products are little varied even with the addition of Zr or Ti+B. So that, the reason why the E_{min} in the weld metal of alloys with additional refining elements in the lower temperature zone of the BTR increase more than those without additional elements is considered because of the remarkable grain refinement by the addition of Zr or Ti+B.

In the case of 5083, it seems that the E_{min} in the lower temperature zone of the BTR is high enough so that the effect of the grain refinement on it is not so remarkable. As to Al-Mg binary alloys, there is evident difference in the effect of grain refinement on the E_M with Mg contents as shown in Fig. 20. The reason in the above is because the dihedral angle of eutectic

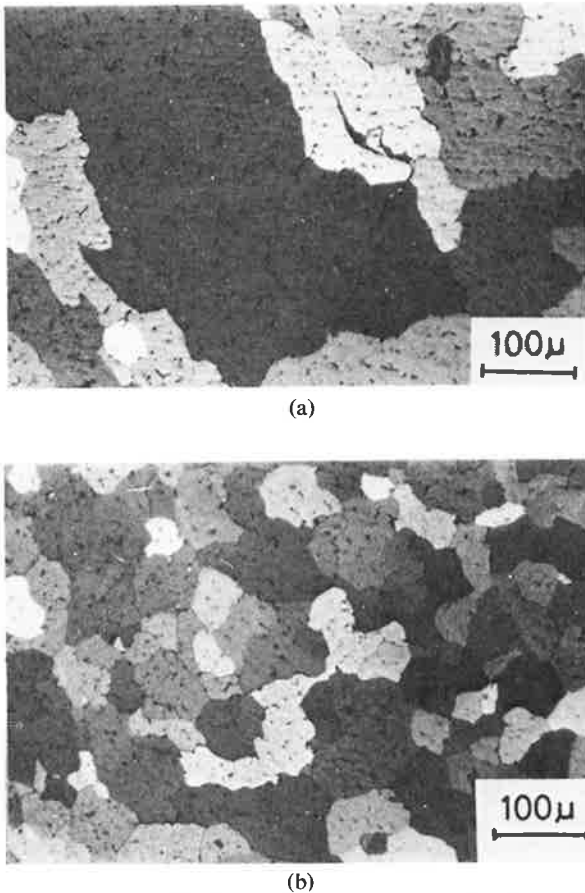


Photo. 5 Examples for macrostructures in weld metals with and without additional refining element (Ti+B) for Al-3 wt% Mg binary alloy
 (a) Al-3.03 wt% Mg
 (b) Al-3.02 wt% Mg with Ti+B

products in the weld metal of alloy (5) (3 wt% Mg) is larger than that of alloy (3) (1 wt% Mg) as shown quantitatively from Photo. 3 (a) and (b).

5. Conclusion

In this study, the new type solidification cracking test has been developed and named Slow-Bending type Trans-Varestraint cracking test. In this cracking test, the strain can be applied on the weld metal during welding with various straining rate. Then, by means of this cracking test, the effect of the straining rate on the properties of ductility in the BTR during welding is investigated for various aluminum alloys. Moreover, some metallurgical properties of weld metal are also investigated in relation to the cracking threshold in the BTR.

The main conclusions obtained are as follows:

(1) The Slow-Bending type Trans-Varestraint cracking test has been developed. In this cracking test, the

strain can be applied on the weld metal during welding with various straining rate. Moreover, it has been made clear that the cracking threshold curve required to cause solidification cracking in the BTR can be obtained by means of this cracking test.

- (2) In most commercially used aluminum alloys except 1070, and Al-Mg and Al-Cu binary alloys, Mg content of which is more than 3 wt% and Cu content of which is about 5 wt%, respectively, the minimum augmented-strain required to cause cracking (E_{min}) in the weld metal tends to vary with the straining rate. That is, when the straining rate is fast as the Trans-Varestraint test, the E_{min} shows the very low value, in general, falling in the range from zero to 0.1%. However, as the decrease of straining rate, the E_{min} is increased in the weld metals of the alloys. As the alloying content is less than that in the above for either binary alloy, the E_{min} is not depended on the straining rate. Moreover, in addition of Ti+B to the Al-1 and -3 wt% Mg binary alloys, the E_{min} is remarkably increased more than those without Ti+B.
- (3) The cracking threshold curve in the weld metal during welding was obtained by exchange the relation between E_{min} and straining rate as mentioned to the one between E_{min} and temperature. The E_{min} in the higher temperature zone of the BTR is very low values, that is, fallen in the range from zero to 0.1% for all the alloys used except commercially pure aluminum alloy, 1070 and alloy (1), the E_{min} of which fallen in the range from 0.1 to 0.3%. Then the E_{min} in the lower temperature zone in the BTR tended to increase in the case of alloys, the E_{min} of which was depended on the straining rate. Consequently, the E_{min} is increased in the lower temperature zone in the BTR with a decrease of straining rate in the weld metal of alloys, Mg content of which is more than 3 wt% and Cu content of which is about 5 wt% for Al-Mg and Al-Cu binary alloys, respectively.
- Also the degree of increase of the E_{min} become larger as the increase of Mg content. Moreover, these tendencies are observed in the weld metals of commercially used aluminum alloys.
- (4) The E_{min} in the lower temperature zone of the BTR is depended on the amount and the dihedral angle of eutectic products in the weld metal. Especially the dihedral angle largely affects on it.
- (5) The addition of Ti+B to the Al-1 and -3 wt% Mg binary alloys remarkably increased the E_{min} in

the lower temperature zone of the BTR more than those without addition of Ti+B and also remarkably refined the grain size in the weld metals. As a result, it is considered that the grain size also affects on the E_{min} in the lower temperature zone of the BTR with slow straining rate.

- (6) The solidification crack susceptibility was evaluated by the CST which obtained from the cracking threshold curve in this investigation. An order of solidification crack susceptibility of the weld metals for each aluminum alloy used is arranged as follows:

for commercially used aluminum alloy;

1070 < (5052, 5083) < 5154 < 2219 < (7N01, 2017)

for Al-Mg binary alloys;

alloy (1) < {alloy (2) (0.5 wt% Mg), (3) (1.0 wt% Mg) and (4) (1.7 wt% Mg)} < alloy (5) (3.0 wt% Mg) < alloy (6) (4.9 wt% Mg)

for Al-Cu binary alloys;

alloy (1) < {alloy (B) (0.8 wt% Cu), (C) (2.0 wt% Cu)} < {alloy (A) (0.5 wt% Cu), (D) (3.0 wt% Cu)} < alloy (E) (5.0 wt% Cu)

These results seem to be agreed with the solidification crack susceptibility in actual welding operation.

Acknowledgement

The authors would like to thank Dr. Toshiyasu Fukui, Sumitomo Light Metal Ind., Ltd. for his offering of the materials and his useful discussion.

References

- 1) Y. Arata, F. Matsuda, K. Nakata and I. Sasaki; "Solidification Crack Susceptibility of Aluminum Alloy Weld Metals (Report I)", Trans. of JWRI, Vol. 5 (1976), No. 2, 53-67.
- 2) T. Senda, F. Matsuda, G. Takano, K. Watanabe, T. Kobayashi and T. Matsuzaka; "Fundamental Investigation on Solidification Crack Susceptibility for Weld Metals with Trans-Varestraint Test", Trans. of JWS, Vol. 2 (1971), No. 2, 1-22.
- 3) Metals Handbook; Vol. 8 (1973), 42.
- 4) O. K. Riegger, L. H. Van Vlack; "Dihedral Angle Measurement", Trans. of AIME, Vol. 218 (1960), October, 933-935.
- 5) Metals Handbook; Vol. 8 (1973), 37.
- 6) M. Chernavski; "Measurement of movement by the weld edges during the solidification of weld metal", Avt. Svarka., 1973, No. 2, 36.
- 7) Y. Arata, F. Matsuda and S. Harada; "Dynamic measurement of deformation behavior near molten puddle during welding of aluminum sheet (in Japanese)", Welding Processes Committee of JWS, No. SW-847-76, July, 1976.
- 8) Pumphrey, W. I. and Lyons, J. V.; "Cracking During the Casting and Welding of the More Common Binary Aluminum Alloys", J. Inst. of Metals, Vol. 74 (1948), 439-455.
- 9) Dowd, J. D.; "Weld Cracking of Aluminum Alloys", W. J., Vol. 31 (1952), No. 2, 488s-456s.